Journal of the Korean Society for Nondestructive Testing
Vol. 22, No. 6 (2002. 12)

Two-Dimensional Numerical Modeling and Simulation of Ultrasonic Testing

Hyunjune Yim† and Eunsol Baek

Abstract As an attempt to further improve the reliability and effectiveness of ultrasonic testing (UT), a two-dimensional numerical simulator of UT was developed. The simulator models the wave medium (or test object) using the mass-spring lattice model (MSLM) that consists of mass-points and springs. Some previous simulation results, obtained by using MSLM, are briefly reviewed in this paper, for propagation, reflection, and scattering of ultrasonic waves. Next, the models of transmitting and receiving piezoelectric transducers are introduced with some numerical results, which is a main focus of this paper. The UT simulator, established by combining the transducer models with the MSLM, was used to simulate many UT setups. In this paper, two simple setups are considered as examples, and their simulated A-scan signals are discussed. The potential of the MSLM, transducer models, and the UT simulator developed in this study to be used in the actual UT is confirmed.

Keywords: ultrasonic nondestructive testing, numerical simulation, mass-spring lattice model, A-scan signal

1. Introduction

One of the most active research areas in ultrasonic nondestructive evaluation (NDE) is the modeling of the physical phenomena involved in the actual ultrasonic testing (UT). This line of research has been demanded by the difficulty often experienced in interpreting the UT results, or by the resulting relatively low reliability of UT. Difficulty in understanding and interpreting the UT results originates from the complexity of the principles governing the wave phenomena involved in UT. Ultrasonic waves in solids do not propagate in such a collimated manner as X-rays; they diffract when they confront with sharp edges; and, they mode-convert when they reflect, refract and diffract, to mention only a few salient features (Graff, 1991; Datta et al., 1990). Simply stated, the physical behavior of ultrasonic waves in solids is often too complex for the average UT practitioner to immediately figure out.

One of the sources to resort to in this situation is computers as their computing capability continues to rapidly increase. Computers may assist the UT practitioner in interpreting what he or she sees on the screen of the equipment in various ways. First, they can produce graphical images of the specimen's inside by utilizing appropriate signal processing and synthesizing techniques (for example, Lorraine (1998)). Secondly, computers, when combined with advanced artificial intelligence techniques, such as neural nets, may help predict the type of defects (Song et al., 1997). Thirdly, using the computer, the physical UT may be simulated (for a few representative examples, see Schmerr (1998), Yim and Sohn (2000), and Yim and Choi (2000)). By

Received October 2, 2002. † Corresponding Author: Department of Mechanical Engineering, Hong-Ik University, Seoul, 121-791, Korea, hjyim@hongik.ac.kr

comparing the measured UT signal with the simulation results for various assumed anomalies, the natures and locations of anomalies may be predicted. This paper is concerned with the third application described above, namely computer simulation of UT.

The ability to accurately simulate UT on computers will not only assist in the interpretation of actual UT measurements, but it can also be used to find the best test configuration and equipment specifications for a new testing task. In addition, such simulation will certainly be a very effective tool in teaching and training UT practitioners. For one or more of these general reasons, or for a similar but much more specific reason, many researchers have attempted to simulate the wave phenomena of UT.

Among them, the authors and their research group have been involved in the development and applications of a numerical model for elastic solids, named the mass-spring lattice model (MSLM), which is based on simple, fundamental physics. The model assumes a lattice structure, which consists of mass-points at the lattice nodes, and springs that connect neighboring mass-points. Using the MSLM, generation, propagation, reflection, refraction, and diffraction phenomena have successfully been simulated (Yim and Sohn, 2000; Yim and Choi, 2000; Yim and Choi, 2001). In addition, a modified version of MSLM was developed to simulate ultrasonic wave phenomena in an anisotropic medium, and it was capable to capture most aspects of such a complex problem (Yim and Lee, 2001). Recently, models for ultrasonic transducers have been devised to develop a complete UT simulator that can predict A-scan signals. The present paper will briefly review previous results, and focus on the transducer models and application examples of the UT simulator.

2. Ultrasonic Testing and Problem Definition

In order to facilitate the reader's understanding, Fig. 1 shows a schematic diagram of a typical setup for pitch-catch contact ultrasonic testing with oblique transducers. The entire system may be thought to consist of two parts, separated by the dashed cascade lines in Fig. 1 and labeled "Equipment" and "Test object", respectively. These two parts are actually in contact with each other although they are shown separated in that figure.

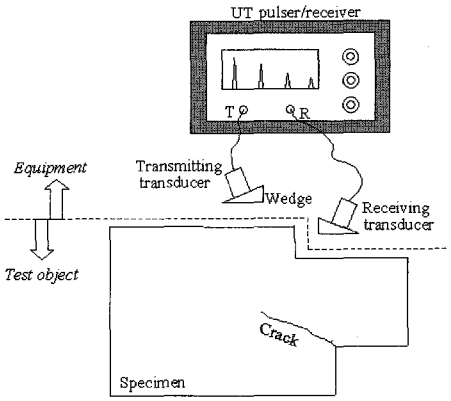

Fig. 1 Schematic diagram of typical ultrasonic testing

An electrical voltage signal generated from the pulser part of the UT pulser/receiver excites the transmitting transducer, and the face of the (piezoelectric) transducer oscillates in response to the electrical signal. This oscillation introduces mechanical waves into the test object or specimen, through a wedge, if any, and a couplant layer. Once introduced into the specimen, the ultrasonic waves propagate in the medium, reflect at boundaries, refract at material interfaces, and diffract at sharp corners. These interactions of the ultrasonic waves with the medium are obviously affected by many aspects of the medium, including those of embedded anomalies. Some of these waves return to the part of specimen's boundary surface that is in contact with the receiving transducer. When excited by these waves (through a couplant layer and a wedge, if any), the piezoelectric transducer produces electric voltage signal, which is fed to the receiver part of the UT pulser/receiver. Then, the oscilloscope shows the received electric voltage signal that is

called the A-scan signal. Information regarding all anomalies must be 'mined' from this A-scan signal, and this task is not always simple and straightforward.

Such division of the entire system into two parts as shown in Fig. 1 is mostly for the simplicity of presentation in this paper, but it also has physical reasons. The physical phenomena occurring in the lower 'Test object' part are all wave behaviors such as propagation, reflection, refraction and diffraction as explained above. The modeling of 'Test object' using the MSLM, for the simulation of wave behaviors, was completed through the previous work (Yim and Sohn, 2000; Yim and Choi, 2000; Yim and Choi, 2001), and it will be briefly reviewed in Section 3 of this paper. In the upper 'Equipment' part, however, several different non-wave types of physical phenomena occur, except for the short-range wave behaviors in couplant layers and wedges. The focus of the present paper lies on the 'Equipment' part, as will be discussed in details in Section 4.

3. Modeling of 'Test Object'

In this section, the MSLM is introduced along with explanations about how boundaries of the specimen and defects are modeled using the model. Some numerical results containing reflected, refracted, and diffracted waves are also presented.

3.1. The mass-spring lattice model (MSLM)

The numerical model, MSLM, used in this work is schematically depicted in Fig. 2 (Yim and Sohn, 2000; Yim and Choi, 2000) that shows only a representative cell containing a center mass-point and its neighboring mass-points along with all springs connecting the outer mass-points to the center. The present version of MSLM is two-dimensional, assuming a state of plane strain in the plane of Fig. 2. Its extension to three dimensions is straightforward, but has been precluded by the potentially high cost of computation time.

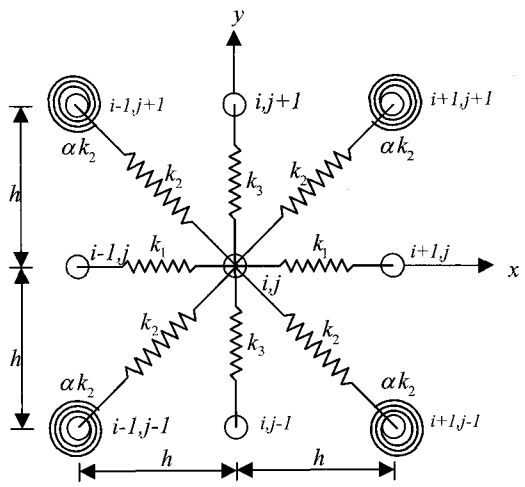

Fig. 2 Schematic diagram showing representative cell of MSLM

When a homogenous and isotropic medium is considered, the mass of each mass-point and the spring constants of both linear and rotational springs in Fig. 2 may be found in terms of the mass density and elastic constants of the material as (Yim and Sohn, 2000)

$$m = \rho h^2, \quad k_1 = k_3 = \lambda + \mu,$$
$$k_2 = \frac{\lambda + 3\mu}{4}, \quad \alpha = \frac{\mu - \lambda}{\lambda + 3\mu} 2h^2 \qquad \cdots\cdots (1)$$

where ρ, λ, and μ are the mass density, and Lame elastic constants of the specimen material, respectively; and, h denotes thelattice spacing. The difference equations to be numerically solved are merely the equations of motion for each mass-point that is subjected to the forces of the springs connected to it. Details may be found in the previous work (Yim and Sohn, 2000; Yim and Choi, 2000; Yim and Choi, 2001).

One of the advantages of MSLM over other numerical methods lies in the simplicity in modeling various material boundaries such as free boundaries, crack faces, and material interfaces. The fact that the MSLM is based on the fundamental physics indeed renders these modeling tasks straightforward. First, free boundaries and crack faces are

modeled simply by disconnecting all springs that intersect with them. Fig. 3 shows an example of modeling a free boundary. Similarly, the material interface may be modeled by assigning the harmonic mean of spring constants in the two materials to the springs that intersect with the material interface (Yim and Choi, 2000).

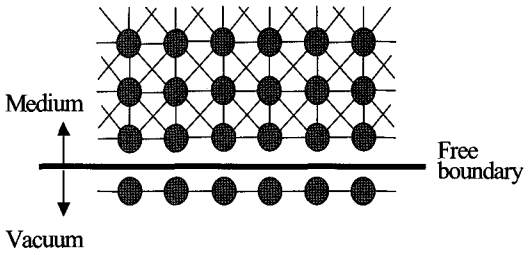

Fig. 3 Method of modeling free boundary using MSLM

3.2. Simulation of Wave Behaviors

As mentioned above, a number of wave phenomena have been simulated using the MSLM. Only a few are shown in this paper to review the previous work. All numerical results in this paper assume that the specimen's material is steel whose material properties are $\rho = 7860 kg/m^3$, $\lambda = 1.11 \times 10^{11} N/m^2$, and $\mu = 8.2 \times 10^{10}\ N/m^2$. Fig. 4 shows computed wavefield generated by a point source. Note here that all wavefield results in this paper, including Fig. 4, display the distribution of displacement magnitudes of mass-points, at a given instant, in a gray scale with black representing no displacement and white the maximum value. The point source assumed for Fig. 4 is an isolated force acting vertically on the mass-point at the center of the medium, varying sinusoidally with time for two cycles. Fig. 4 exhibits both longitudinal (P) and shear (SV, or simply S) waves emanating circularly from the source. The wavespeeds of both waves, computed from Fig. 4, coincide with the analytical values. Similarly, wavefields emanating from a line source, consisting of point sources distributed along a straight line, were computed. Though not shown here, it formed a plane P (or S) wave (Yim and Sohn, 2000).

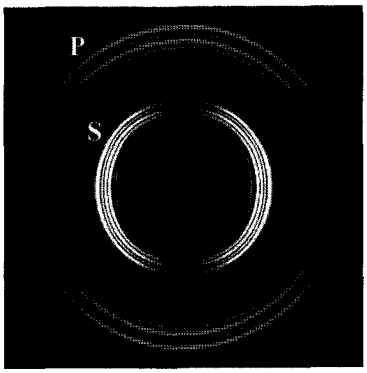

Fig. 4 Simulated wavefield showing longitudinal and shear waves generated by point source

Considering such a plane wave from a line source as the incident wave, its reflection, refraction, and diffraction were studied (Yim and Sohn, 2000; Yim and Choi, 2000; Yim and Choi, 2001). For example, Fig. 5 is concerned with reflection of incident plane P wave from a horizontal free boundary. As shown by the schematic diagram in Fig. 5(a) and by the computed wavefield in Fig. 5(b), the incident P wave reflects from the free boundary with mode conversion; that is, both P and S waves are produced upon reflection, in agreement with the wave physics. Both angles of reflection for the two reflected waves were measured from the numerical result, and they closely coincided with the corresponding analytical values.

Finally, the phenomenon of diffraction of ultrasonic waves from a crack tip was studied, one example of which is shown in Fig. 6. The wavefield in Fig. 6(b) is a result of simulation for the problem schematically depicted in Fig. 6(a), that is, the problem of a plane P wave being obliquely incident on a vertical crack. As may be seen in Fig. 6(b), two diffracted waves one longitudinal and the other shear are generated at the crack tip and propagate in all directions.

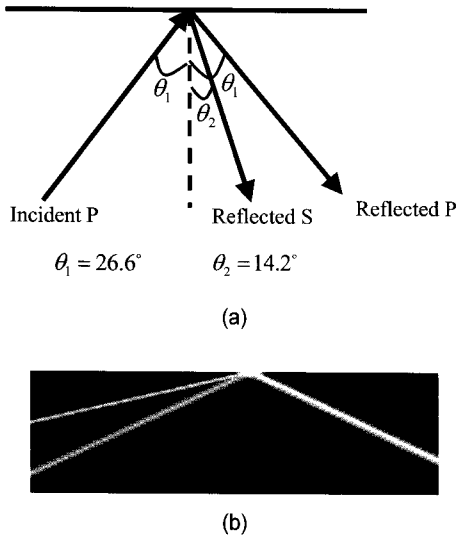

Fig. 5 Simulation of reflection of plane P wave from free boundary: (a) schematic diagram of wave rays, and (b) simulated wavefield exhibiting mode conversion

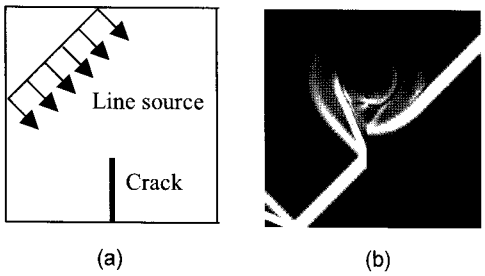

Fig. 6 Simulation of diffraction of plane P wave from crack tip: (a) schematic diagram of the problem, and (b) simulated wavefield showing two diffracted waves

4. Modeling of 'Equipment'

This section describes the results of recent research on the modeling of the 'Equipment'part in Fig. 1. Instead of attempting to model the details of the electric circuits in the flaw detector, cables, various components of each transducer (Silk, 1984), the modeling approach presented here focuses on the transmission of mechanical waves between the transducers and the 'Test object'.

4.1. Modeling of Transmitting Transducer

As mentioned above, only the end effect of a transmitting transducer, that is, the process of introducing mechanical waves into the specimen, is modeled. Fig. 7 is a schematic diagram showing such a model. The effect of all equipment including the transducer and wedge is modeled as a distribution of traction, $\mathbf{T}(x,t)$, distributed only on the excited portion of the specimen's boundary surface. The function, $\mathbf{T}(x,t)$, is set equal to the traction of a plane wave having a desired mode and direction: for example, a 30°-oblique plane S wave. This amounts to assuming that a finite-width plane wave generated by the piezoelectric element of the transducer has propagated through the wedge and couplant, and excites the boundary of specimen.

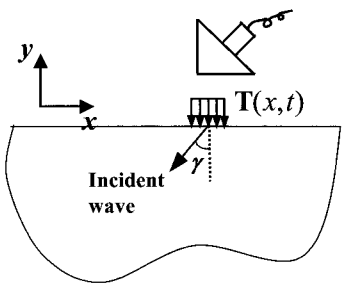

Fig. 7 Modeling of transmitting transducer in MSLM

Though the time dependence of $\mathbf{T}(x,t)$ should be pulse-like, the traction for steady-state time-harmonic plane waves is first considered, which will later be used for frequency synthesis. Mathematical expressions for such (plane wave) traction, $\mathbf{T}(x,\omega)$, for P and S transducers may be derived, respectively, as (Bostrom and Wirdelius, 1995)

$$\mathbf{T}(x,\omega) = Agi\mu k_p\left[(k_s^2/k_p^2 - 2\sin^2\gamma)\mathbf{e}_y + \delta\sin 2\gamma\mathbf{e}_x\right]e^{-ik_p x\sin\gamma} \quad \cdots\cdots (2)$$

and

$$\mathbf{T}(x,\omega) = Agi\mu k_s\left[\sin 2\gamma\mathbf{e}_y - \delta\cos 2\gamma\mathbf{e}_x\right]e^{-ik_s x\sin\gamma} \quad \cdots\cdots (3)$$

where the time dependence, e^{-iwt}, has been omitted; A is the amplitude of displacement of the plane harmonic wave; $g(x)$ is a function used for non-uniform distribution of traction along the surface of specimen; $i=\sqrt{-1}$; μ is the shear modulus of the specimen material; k_p and k_s are the wave-numbers of P and S harmonic waves, respectively; γ defines the propagating direction of the incident wave (see Fig. 7); $\mathbf{e}_x$ and $\mathbf{e}_y$ are the unit vectors in the x and y directions, respectively; and, δ is a constant, named the 'shear transmission factor', ranging between 0 (zero) and 1, depending on the effectiveness of shear force transmission or essentially on the viscosity of the liquid couplant.

Since the electrical voltage input to the transmitting transducer may be assumed to be impulsive, the time-domain expressions for $\mathbf{T}(x,t)$ may be found by synthesizing the frequency spectrum, given by eqn. (1) or (2), with a 'weighting function' given by the frequency-domain characteristic of the transducer. That is,

$$\mathbf{T}(x,t) = \mathsf{F}^{-1}\{\mathbf{T}(x,\omega)S_t(\omega)\} \quad \cdots\cdots\cdots (4)$$

where $S_t(\omega)$ is the frequency-domain characteristic of the transmitting transducer, and F^{-1} denotes the inverse Fourier transform. The frequency function, $S_t(\omega)$, usually assumes the form of a band-pass filter, characterized by the center frequency and bandwidth.

In the MSLM, the traction calculated by eqn. (4) is applied to the mass-points along the excited region of the boundary surface of specimen. Though many cases were studied, only two examples of transmitting transducers are presented in this paper: a normal transducer, and an oblique transducer. Fig. 8 shows a snapshot of simulated wave field radiated from a normal P transducer (without a wedge), attached to the top surface of the medium and having a center frequency of 2.0 MHz and 6 dB bandwidth of 2.0 MHz. In the computations to yield Fig. 8, eqn. (2) was used with parameters set as A=1.0, γ=0, and $g=\sqrt{a^2-x^2}$ where a is the radius of the transducer and the origin of x is located at the center of the transducer. The g-function was defined as such in order to suppress theedge waves by smoothing out the ends of the excitation. It may be observed from Fig. 8 that strong 'planar' P wave has been radiated from the transducer at the top surface, and has propagated vertically downward. Two edge waves, P and S, emanating circularly from each end of the 'transducer' are also observed in Fig. 8.

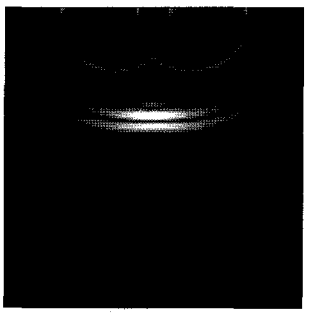

Fig. 8 Simulated wavefield, radiated from normal P transducer

When an oblique transducer (i.e. nonzero γ) is considered, the exponential terms in eqns. (2) and (3) exist, unlike in the case of normal transducers (i.e. vanishing γ). These exponential terms, when combined with the omitted time function, e^{-iwt}, simply represent harmonic waves propagating in the negative x-direction with a wavenumber of $k \sin\gamma$. This means that different points on the boundary are excited harmonically with different time lags. Recognizing this and implementing such time lags for all excited mass-points in the MSLM may yield numerical results for oblique transducers. One example is shown in Fig. 9 which is for a 45°-oblique S transducer having a center frequency of 1.5 MHz and 6 dB bandwidth of 1.5 MHz. Eqn. (3) was used to produce Fig. 9, with its parameters set as A=1.0, γ=45°, δ=1.0, and $g=\sqrt{a^2-x^2}$. Fig. 9 shows a strong shear wave inclined 45 with respect to the horizontal, weak surface waves behind the S wavefront, and a weak P edge wave emanating circularly from the right end of the excited region.

Fig. 9 Simulated wavefield, radiated from 45°-oblique S transducer

The numerical results in Figs. 8 and 9, and others not shown here were compared with the results in (Bostrom and Wirdelius, 1995) that contains analytically computed wavefields using the same (but three-dimensional) formulation as that in the present work. Because of the difference in their dimensionality, only the results in (Bostrom and Wirdelius, 1995) in the *x*-*y* plane (see Fig. 7) were compared with the results in the present work. All comparisons showed good qualitative agreements, though they did not match exactly due to the plane-strain assumption of the present two-dimensional study.

4.2. Modeling of Receiving Transducer

A piezoelectric transducer used for reception of ultrasonic waves may be assumed to generate electrical voltage in proportion to the wave-induced traction acting on its face. In most cases, however, the traction at a point on the transducer's face differs from that at another point. Therefore, it is reasonable to consider the average traction across the transducer's face. Furthermore, the contribution of traction in generating the electrical voltage may depend on the location of the traction on the transducer's face. Considering all these aspects, the average traction on the face of a normal receiving transducer (see Fig. 10) may be computed, in the MSLM, as

$$T_{avg}(t) = \frac{\sum_{j=1}^{N} g^j f_y^j(t)}{N h} \qquad \cdots\cdots\cdots (5)$$

where N is the number of contributing mass-points on the specimen's boundary surface; $f_y^j(t)$ is the net vertical spring force exerted on the *j*th mass-apoint by the inside of the medium; and, g^j is a discretized expression for the function $g(x)$ in eqns. (3) and (4). It has been assumed that the receiving transducer is only sensitive to the traction component normal to its face.

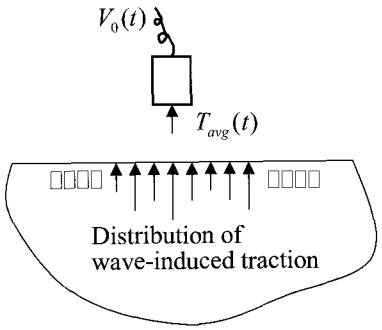

Fig. 10 Modeling of normal receiving transducer in MSLM

When an oblique transducer is used for the reception of ultrasonic waves, the wedge located between the receiving transducer and specimen causes time delays in eqn. (5) as required by the extra travel distances of waves in the wedge (see Fig. 11). A simplified model is used in this study, which assumes that all waves other than the direct P waves through the wedge - shown in Fig. 11 as oblique arrows, or rays, in the wedge - do not effectively excite the transducer face. It is obvious from Fig. 11 that the amount of time delay is different from ray to ray. Therefore, for oblique receiving transducers, eqn. (5) should be modified to

$$T_{avg}(t) = \frac{\sum_{j=1}^{N} g^j f_y^j(t - j\Delta - \Delta_0)}{N h} \qquad \cdots\cdots (6)$$

where Δ is the relative time delay between two adjacent rays in Fig. 11, and Δ_0 is the minimum time delay experienced by the shortest ray, drawn for the leftmost mass-point in Fig. 11. From simple geometrical analysis, it may be found that

$$\Delta = \frac{h \sin \gamma^w}{c_p^w} \qquad \cdots\cdots\cdots (7)$$

where c_p^w is the P wave velocity in the wedge, and γ^w is the angle of wedge defined in Fig. 11.

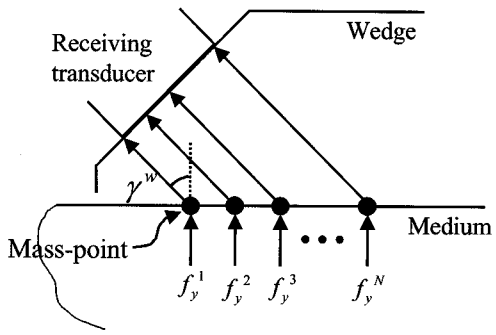

Fig. 11 Simplified model of oblique receiving transducer in MSLM

Once the average traction on the transducer face is calculated by eqn. (5) or eqn. (6), it should be converted to electrical voltage output, $V_0(t)$. The conversion will not be equally responsive to all frequency components of the average traction, but it will be affected by the characteristics of the transducer, electronic circuits in the receiver part, and cables. To consider this effect, first, the average traction is Fourier transformed; secondly, it is multiplied by the frequency-domain characteristics of the receiving transducer (and, circuits and cables); and then, finally, it is inverse-transformed to obtain the time-domain function. This process implies that the frequency-domain characteristicsof the receiving transducer play a role as a filter (most ften, a band-pass filter) in the conversion process. This idea may mathematically be expressed as

$$V_0(t) = \mathsf{F}^{-1}\{T_{avg}(\omega)S_r(\omega)\} \quad \cdots\cdots (8)$$

where $T_{avg}(\omega)$ is the Fourier transform of $T_{avg}(t)$ calculated by eqn. (5) or eqn. (6), and $S_r(\omega)$ is the frequency-domain characteristics of the receiving transducer, electric circuit, and cable. Numerical results obtained by using this model are not shown in this section because the results presented in the following section involve its use.

5. Examples of UT Simulation

Combining all the models developed as described in the previous sections, a complete UT simulator was established. Using the simulator, several canonical UT problems were simulated to obtain the A-scan signals. Only two cases are illustrated in this paper.

Fig. 12 shows a simple setup for typical pitch-catch tests, where incident waves from the right-hand transmitter are reflectedfrom the bottom face of the specimen having a thickness of T, and the reflected waves are received by the left-hand transducer. The two transducers are both assumed to be 45°-oblique S transducers having identical specifications. When the spacing, d, between the two transducers is equal to $d_0 = 2T \tan\gamma = 2T$, the radiated ray from the center of the transmitting transducer reaches, after reflection, the center of the receiving transducer. (Note here that the incident angle of 45° exceeds the critical angle for steel, so there is no P reflected wave.) Therefore, it is clear that when $d \neq d_0$, the received A-scan signal will be reduced because the 'catcher' will then miss the most significant portion of the reflected wave energy.

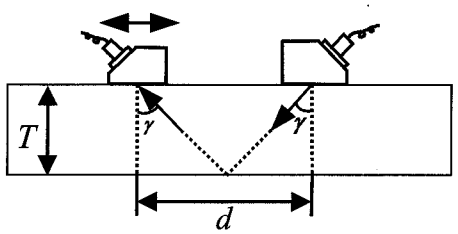

Fig. 12 Setup for typical pitch-catch test

Using the UT simulator developed in this study, this problem was simulated with various values of d. Examples of numerical results are shown in Fig. 13. The three curves are respectively for $d = d_0$, $d = d_0 + a$, and $d = d_0 - 2a$ (a may be an arbitrary length, and it was taken here to be the radius of the transducer), and they are all shown in one plot for easy comparison. No

numerical values, except zeroes, are labeled on the vertical axis of these plots because the plots are overlapped and, more importantly, because the values will not have physical meaning until calibration is made through comparisons with experiments. Two aspects are immediately noticeable from Fig. 13. First of all, as expected above, when $d \neq d_0$, the received A-scan signals are significantly smaller than that in the case of $d = d_0$. Secondly, it may be observed that as the inter-transducer spacing increases, the time of flight for the reflected wave increases, as may easily have been expected.

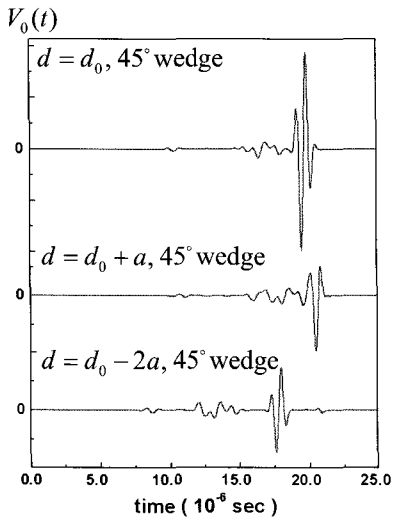

Fig. 13 Simulated A-scan signals in theproblem of Fig. 12, for various values of spacing between transmitting and receiving transducers

As a second example, consider a typical setup for pulse-echo testing for detection of cracks, epicted in Fig. 14. Suppose the location of the transducer is fixed, with the horizontal spacing between the crack and the center of the transducer being $d = d_0 = T$. When a 45°-wedge is used, the ray from the center of the transducer will be directed toward the root of crack, and most other rays will be reflected twice (from the bottom face of specimen, and from the right-hand face of the crack) and be directed back to the transducer, as indicated by the dot-dashed lines in Fig. 14. If a wedge labeled an angle different from 45° is used, most of incident waves will be directed away from the paths in Fig. 14 so that much less or no reflected waves will return to the transducer. This prediction is confirmed by the numerical results in Fig. 15. That is, the A-scan signal for 70°-wedge is much smaller than that for 45°-wedge. Though they will have to be verified by experiments, the A-scan signals in Figs. 13 and 15 as well as others not shown here resemble in shape the results obtained from other models and experiments (Schmerr, 1998).

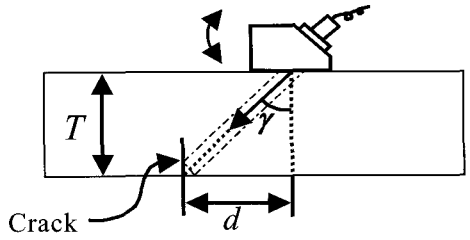

Fig. 14 Setup for typical pulse-echo test for crack

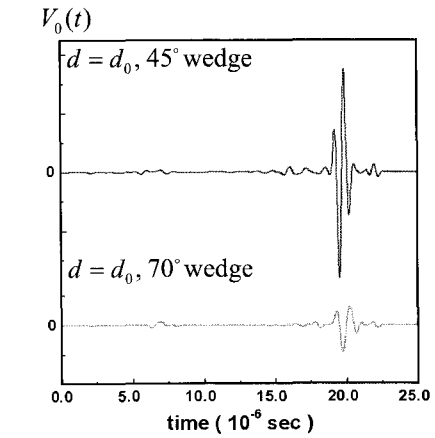

Fig. 15 Simulated A-scan signals in the problem of Fig. 14, for two different angles of wedge

6. Conclusions

A computer simulator for UT was developed by combining the previously developed MSLM and recently developed models for transducers. Simulated wavefields obtained by using the MSLM

and transducer models were illustrated to show their agreements with wave physics. Also, the A-scan signals computed from the UT simulator were presented for two simple examples of typical UT setup. It was observed that as the parameters of the setup change, the magnitude and time of flight of the A-scan signals vary in the predicted directions. Furthermore, it was observed that the profile of the computed A-scan signals resembles those from other modeling studies and experiments.

Several modifications of the simulator are required for more accurate and reliable simulation of actual UT. First, each of the MSLM and transducer models should be verified by experiments. Because the numerical model is two-dimensional, the experiments will have to be set up accordingly so that the conditions for plane strain states are met. Or, the models will have to be extended to three dimensions before they are verified by the usual (three-dimensional) experiments. Secondly, the model for the receiving transducer needs to be further developed, particularly by incorporating the wave phenomena in the wedge. Third, it may be interesting and useful to develop an MSLM for fluid, and include it for the couplant layers in the transducer models. Once all these improvements have beenmade along with experimental verifications, the UT simulator, initially established in this work, will play important roles in enhancing the reliability and effectiveness of ultrasonic testing.

Acknowledgments

This work was supported by the Safety and Structural Integrity Research Center sponsored by the Korea Science and Engineering Foundation.

References

Bostrom, A, and Wirdelius, H. (1995), "Ultrasonic probe modeling and nondestructive crack detection", Journal of the Acoustical Society of America, Vol. 97, No. 5, pp. 2836-2848

Datta, S. K., Achenbach, J. D., and Rajapakse, Y. S. (1990) Elastic Waves and Ultrasonic Nondestructive Evaluation, North-Holland, Amsterdam

Graff, K. F. (1991) Wave Motion in Elastic Solids, Dover, New York

Lorraine, P. W. (1998) "Laser Ultrasonic Imaging of Lamb Waves in Thin Plates", Nondestructive Characterization of Materials, Vol. 8, Ed. R. E. Green, Jr., pp. 67-72

Schmerr, Jr., L. W. (1998) Fundamentals of Ultrasonic Nondestructive Evaluation, Plenum, New York

Silk, M. G. (1984) Ultrasonic Transducers for Non-destructive Testing, Adam Hilger, Bristol

Song, S. J., Kim, H. J., Choi, S. H., and Lee, J. H. (1997) "Classification of Surface Flaws in Cold-Rolled Steel Plates Using Probabilistic Neural Network", Journal of the Korean Society for Nondestructive Testing, Vol. 17, No. 3, pp. 162-173 (in Korean)

Yim, H. and Choi, Y. (2000) "Simulation of ultrasonic waves in various types of elastic media using the mass spring lattice model", Material Evaluation, Vol. 58, No. 7, pp. 889-896

Yim, H, and Choi, Y (2001) "Simulation of Two-dimensional Propagation and Scattering of Ultrasonic Waves on Personal Computers", Review of Quantitative Nondestructive Evaluation, Vol. 20, Eds. D. O. Thompson and D. E. Chimenti, pp. 59-64

Yim, H., and Lee, C. (2001) "A Computer Model for Ultrasonic Wave Scattering from Cracks in Welds", Proceedings of MPA-SAFE Workshop on Safety Evaluation of Nuclear Power Plant Components, SAFE, Korea, pp. 1-10

Yim, H. and Sohn, Y. (2000) "Numerical simulation and visualization of elastic waves using mass-spring lattice model", IEEE Trans. on UFFC, Vol. 47, No. 3, pp. 549-558

Guide for Authors

Preparation of Manuscripts

General

The contents of manuscripts must be original, previously unpublished elsewhere. Each manuscript should be accompanied by a cover letter indicating that it is original and unpublished and is not being considered for publication elsewhere. A completed KSNT Copyright Form must accompany the manuscript for the review process to begin. For details related to the copyright issue, consult the Copyright section below. The manuscript must be written in English, and a minimum level of English proficiency is required.

The manuscript should include the title of paper, name and affiliation of author(s), an abstract with a few keywords, main body, acknowledgment (if applicable), references, appendices (if applicable), tables, and figures, in the order listed. The main body may consist of introduction, theory or background, experiments, results, discussion, and conclusion(s). All pages should be numbered.

Authors

Complete address including zip or postal code and e-mail address of each author should be provided, with the corresponding author clearly identified.

Abstract

The abstract of 100-150 words must be accompanied by four to six keywords, representing the contents of the paper.

Typesetting of text

The manuscript should be printed on one side of white A4- or letter-sized paper. Text should be double spaced with sufficient margin at each side. The font size of 11 or 12 points is recommended. Use of SI units is strongly recommended. Any non-standard abbreviation should be defined the first time they occur.

Equations

All equations must be written clearly and legibly. Place each equation on a separate line and number the equations sequentially by numbers enclosed in parentheses. Equations must be referred to in the text as, for example, eqn. (1) , or eqns. (1) and (2) , or eqns. (1) through (3) .

References

List all bibliographical references at the end of the main body. They should be arranged alphabetically by the first author and for each author chronologically. Examples of acceptable reference formats for periodicals and monographs are as follows:

Dang, C. and Schmerr, L. W. (2001) Complete Modeling of an Ultrasonic NDE Measurement System An Electroacoustic Measurement Model, Journal of the Korean Society for Nondestructive Testing, Vol. 21, No. 1, pp. 1-21

Rose, J. L. (1999) Ultrasonic Waves in Solid Media, Cambridge University Press, Cambridge, UK, pp. 177-199

Fink, M. (2001) Time Reversed Acoustics, in: D.O. Thompson and D.E. Chimenti (Eds.), Review of Progress in Quantitative Nondestructive Evaluation, Vol. 20A, American Institute of Physics, Melville, New York, pp. 3-15

To cite them in the text, write the surname of the author in parentheses followed by the year of the publication of the reference is given, (Dang and Schmerr, 2001), for example. In case there are several publications by the same author in the same year, use notations 2001a, 2000b, etc. Up to two authors can be mentioned in the text references ; three or more authors should be shortened to the name of the first author with et al.

Tables and figures

References may be followed by Tables and then by Figures, if any. A separate list of Tables and/or Figures caption should be provided. Printing more than one Figure on a page is allowed, but the Figures must be clearly separated with sufficient margin between them. Tables and Figures must be numbered separately, with captions beginning with, for example, Fig. 1 and Table 1, respectively. They should be referred to in the text as, for example, Fig. (or Table) 1, Figs. (or Tables) 1 and 2, or Figs. (or Tables) 1 through 3. Make sure that the size of lettering on Figures is not too small. Images including photographs and micrographs are recommended in high contrast, black and white, and glossy prints. Micrographs should include scale bars for reading magnification. Color reproduction is available when they are vital for readers understanding, but the reproduction cost will be charged to the authors.

Copyright

It is required to transfer the copyright to publish your paper in the Journal. Please fill out the KSNT Copyright Form, and enclose it when submitting the manuscript. To use any material published previously, the author(s) must obtain the permission from the owner (the publisher and/or author) of the rights to the materials. It is the authors responsibility to obtain any permission necessary to use the copyrighted material in his/her manuscript.

Review Process and Page Charges

All manuscripts are subject to strict peer review with respect to their technical quality, clarity, and conformance to the Journal rules. During the review process, all questions and comments of Reviewers and the Editor must be addressed and reflected in the revision of manuscripts by the author(s), and resubmitted within two (2) months. Any revised manuscript submitted later than this period will be considered as a totally new submission. For the final version of manuscripts, an electronic version of the text and the Tables and Figures if possible are required to accompany the hard-copy version. All common formats of computer media (floppy, Zip and CD-ROM) can be used. After a paper is accepted for publication, galley proof will be sent to the corresponding author for the final correction of typesetting errors, which must be returned within five (5) working days of receipt. The author(s) will be invoiced for 200,000 KRW up to ten (10) Journal pages, and 30,000 KRW for each additional Journal page. Once the invoice is fully paid, the corresponding author will be entitled to thirty (30) offprints of the paper and a complimentary copy of the Journal. Additional offprints may be ordered at the time of proofs.

Submission of Manuscripts

Submit all the followings for the review process to begin.

1. Four copies of the manuscript, including one original.
2. A completed KSNT Copyright Form
3. All original photographs, if any
4. All copyright permission letters, if necessary

The package including all the above should be mailed to:

Korean Society for Nondestructive Testing
Attn: JKSNT Publications
1473-10 Seocho-3dong, KID Bldg.
Seocho-ku, Seoul 137-073 Republic of Korea

or

Professor Oh-Yang Kwon
Editor-in-chief, JKSNT
Department of Mechanical Engineering
Inha University
253 Yonghyun-dong, Inchon 402-751
Republic of Korea

Details and Further Inquiries

More information for authors may be found at the Internet site, http://www.ksnt.or.kr. All questions and comments regarding the contents, the style and formats of your paper should be addressed to:

Korean Society for Nondestructive Testing
1473-10 Seocho-3dong, KID Bldg.
Seocho-ku, Seoul 137-073
Republic of Korea
Telephone: + 82-2-583-7564
Fax: + 82-2-582-2743
E-mail: ksnt@unitel.net